Wing Laminar Boundary Layer in the Presence of a Propeller Slipstream

Stan J. Miley*
Texas A&M University, College Station, Texas
Richard M. Howard†
U.S. Naval Postgraduate School, Monterey, California
Bruce J. Holmes‡
NASA Langley Research Center, Hampton, Virginia

The effects of a propeller slipstream on the wing laminar boundary layer have been investigated. Hot-wire anemometer velocity sensor measurements have been performed in flight and in a wind tunnel. It is shown that the boundary layer cycles between a laminar state and a turbulent transitional state at the propeller blade passage rate. The cyclic length of the turbulent transitional state increases with decreasing laminar stability. Analyses of the time-varying velocity profiles show that the turbulent transitional state has characteristics similar to relaminarizing flow and laminar flow with external turbulence. Trends indicate that laminar flow design principles applied to the airframe affected by the propeller slipstream can have beneficial results.

Nomenclature

c = airfoil chord length
H_{12} = boundary layer momentum thickness parameter $= \dfrac{\delta_1}{\delta_2}$
H_{32} = boundary layer energy thickness parameter $= \dfrac{\delta_3}{\delta_2}$
Re_c = chord Reynolds number
U = local mean velocity in the streamwise direction
x = distance along airfoil chord
y = transverse coordinate
α = airfoil angle of attack
δ = boundary layer thickness, $U/U_e = 0.995$
δ_1 = boundary layer displacement thickness $= \int_0^\infty [1-(U/U_e)]\mathrm{d}y$
δ_2 = boundary layer momentum thickness $= \int_0^\infty (U/U_e)[1-(U/U_e)]\mathrm{d}y$
δ_3 = boundary layer energy thickness $= \int_0^\infty (U/U_e)[1-(U/U_e)^2]\mathrm{d}y$

Subscripts

e = boundary layer edge value
∞ = freestream value

Introduction

IT is becoming increasingly apparent that natural laminar flow (NLF) is a technology whose time has come to the general aviation industry. Laminar flow, which had been the exclusive province of high-performance sailplanes, is now commonplace in sport aircraft and is appearing on high performance, advanced technology prototype business aircraft. The adoption of NLF methodology brings numerous design problems in the general area of aerodynamic cleanliness. An important design problem for propeller-driven aircraft is where to put the propeller, or more to the point, what to do about the heretofore apparent adverse effects of the propeller slipstream. Tractor propeller installations offer many advantages. A generally accepted disadvantage, however, is that the propeller slipstream will come into contact with some parts of the airframe and eliminate the beneficial effects of laminar flow from the affected areas. The commonly applied solution is to adopt pusher installation designs to remove the slipstream from contact with the airframe. Pusher installations have their disadvantages also, however. Increased propeller vibration and noise from wake cutting by the propeller blades is a common problem.

In a recent survey of propeller propulsion integration technology by Miley and von Lavante,[1] no clear advantage was found in the comparison of tractor vs pusher wing mounted installations. This evaluation is based upon a review of available published data from 1930 to the present. A clearer view was needed on the effect of propeller slipstreams on laminar flow.

The early flight and wind tunnel investigations of laminar wing boundary layers within propeller slipstreams were conducted by Young and Morris[2,3] and Hood and Gaydos.[4] These researchers concluded from their limited investigations that the propeller slipstream caused the point of laminar/turbulent transition to move forward to a location near the wing leading edge. High-speed flight investigation results by Zalovcik[5] and Zalovcik and Skoog[6] describe wing boundary layer measurements in propeller slipstreams on two different P-47 aircraft, one utilizing an NACA 230 series wing section and the other an NACA 66 series laminar flow wing section. Their results showed little effect of the slipstream on transition for the NACA 230 section; however, the test with the NACA 66 series section resulted in the transition point location moving forward from 50 to 20% chord. The general consensus from this early work is that the propeller slipstream reduced or eliminated the extent of laminar flow by forcing transition to occur earlier.

Received Dec. 21, 1986; revision received Oct. 26, 1987.

*Associate Professor, Aerospace Engineering Department; currently Guest Scientist, Institut für Entwurfsaerodynamik, German Aerospace Research Establishment, DFVLR, Braunschweig, West Germany. Member AIAA.
†Assistant Professor, Department of Aeronautics. Member AIAA.
‡Chief, Flight Applications Branch. Senior Member AIAA.

Recent work by Holmes, Obara, and Yip[7] and Holmes, et al.[8] brought into question the validity of the earlier measurement methods for accurate determination of transition in propeller slipstreams. Time-dependent behavior, particularly at frequencies associated with propeller blade passage rate, was not measurable by the low-frequency response pressure probe methods commonly employed at that time. Measurements by Holmes, et al.[7] using surface hot-film sensors indicated the existence of a cyclic, turbulent behavior resulting in convected regions of turbulent packets between which the boundary layer appeared to remain laminar. This behavior is shown in Fig. 1, taken from Ref. 7.

More recently, detailed investigations were conducted in the laminar boundary layer in the presence of a propeller slipstream. Hot-wire sensors were used to provide time histories of the laminar/turbulent state, and of the time-dependent boundary-layer velocity profiles. Measurements were performed in a small wind tunnel and in flight on a light twin aircraft. These data provide a more complete physical description than has previously existed of laminar boundary layer behavior in near-field propeller slipstreams.

Experimental Investigations

Initial Flight Experiments

Initial flight measurements of the wing boundary layer within the slipstream were made on a Gulfstream Aerospace GA-7 Cougar at two chord locations using dual-probe hot-wire anemometer velocity sensing system. The GA-7 is a light, twin-engine, four place, piston-engine propeller-driven airplane. The chordwise probe locations are shown in Fig. 2. One probe was located well within the boundary layer, and the other was located directly above the external flow. The airfoil section of the wing is modified NACA 63 series. A favorable pressure gradient was assumed to exist back to the 30% chord location for the low angle of attack cruise flight regime. Flow visualization studies confirmed regions of laminar flow extending aft to this location. Data were recorded over the entire flight speed range of the aircraft.

The results from this initial investigation are given in Figs. 3–6. The signal traces presented in the figures are time histories of the local flow velocities in the boundary layer and in the external flow. Figure 3 gives a physical picture of the probe location with respect to the laminar and turbulent profile shapes. Figure 4 is a conceptual sketch of the velocity signal behavior and is provided to identify the important features indicated by the data. The actual character of the traces will be described shortly.

Figures 5 and 6 must be viewed in relation to Figs. 3 and 4. Figure 5 gives the data with the probes located at 12% chord. The external flow probe sensor was damaged during takeoff and only the boundary layer sensor remained in operation. In the five pictures in the upper part of the figure, the boundary layer velocity signal shows a periodic laminar/turbulent behavior. The locally cyclic turbulent flow periodically increases the mean velocity seen by the probe because of the fuller turbulent profile at the probe height above the surface. The length of time during which the cyclic turbulence traverses a station in the boundary layer is dependent upon the level of laminar stability which varies with pressure gradients as speed changes. At the high-speed end, the pressure gradient is strongly favorable, and laminar stability is correspondingly high. Here, the boundary layer reverts almost immediately back to laminar flow after the passage of the external disturbance. At the low-speed end, the pressure gradient is no longer strongly favorable, laminar stability is greatly decreased, and the turbulence remains for almost the total cycle.

The three pictures in the lower part of the figure show the boundary layer behavior with the propeller stopped. The aircraft was flown with one engine for this sequence. The pictures show laminar, transitional, and turbulent flow corresponding to the airspeed range. The laminar signal is not a pure flat d.c. signal as one would expect. There is a small sinusoid superimposed due to the vibration inherent in propeller-driven aircraft. This effect was verified by changing engine speed and observing the frequency change in the wave form.

Figure 6 presents the data with the probes located at the 30% chord location. In the external flow, the nature of the velocity disturbance from the propeller is evident. The effect of reduced laminar stability at the 30% chord location is evident from the lengthened turbulent regions appearing inside the boundary layer in the pictures. The viscous blade wake appears as a short-wave impulse discernible in the external flow at the higher-speed conditions. As the airspeed is reduced, the propeller blade operates at an increasingly higher angle of attack

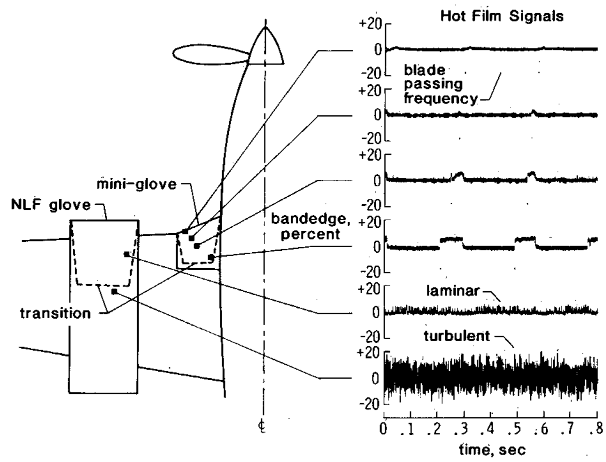

Fig.1 Time-dependent slipstream effects on T-34C aircraft.[7]

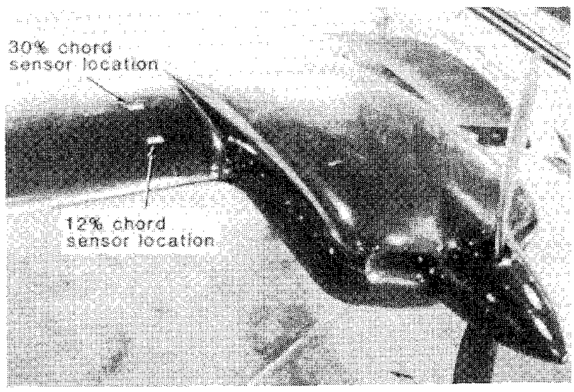

Fig. 2 Sensor locations on Gulfstream Cougar aircraft, 12 and 30% chord.

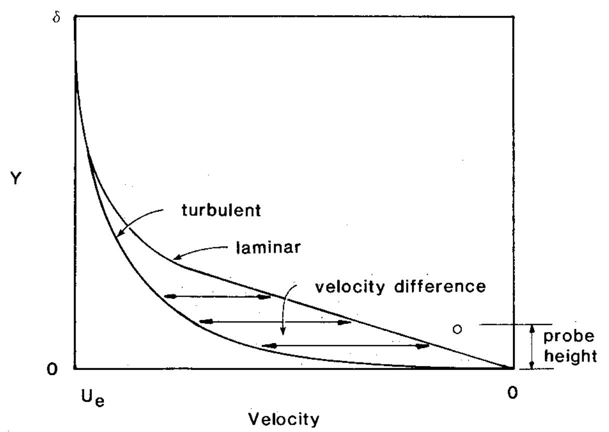

Fig. 3 Velocity profile comparison showing hot-wire probe location.

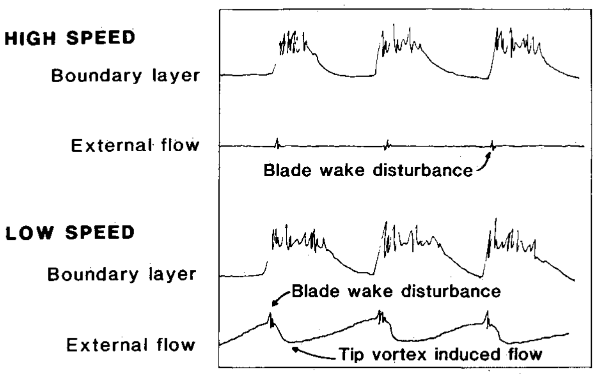

Fig. 4 Conceptual sketch of hot-wire velocity signals.

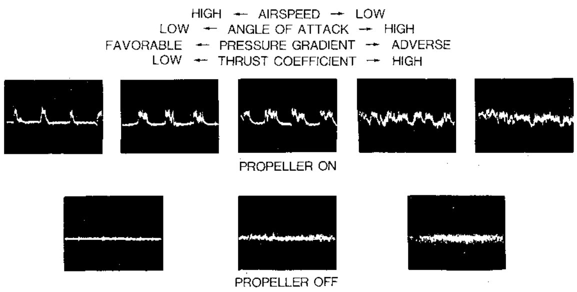

Fig. 5 Time-dependent velocity signals in boundary layer on Gulfstream Cougar aircraft: 12% chord location in propeller slipstream.

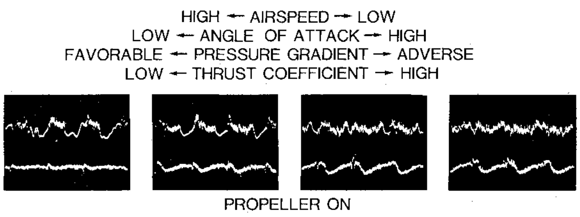

Fig. 6 Time-dependent velocity signals in boundary layer and in external flow on Gulfstream Cougar aircraft: 30% chord location in propeller slipstream.

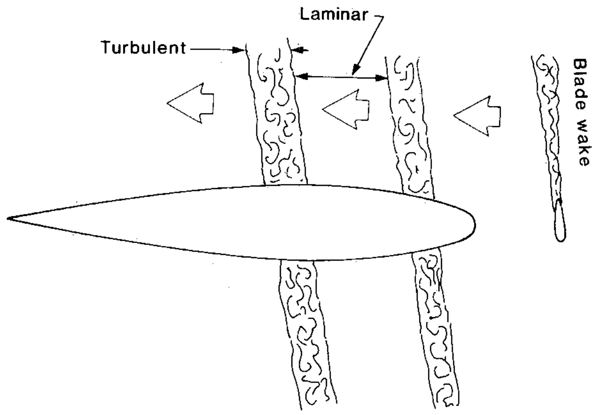

Fig. 7 Slipstream disturbance flow model.

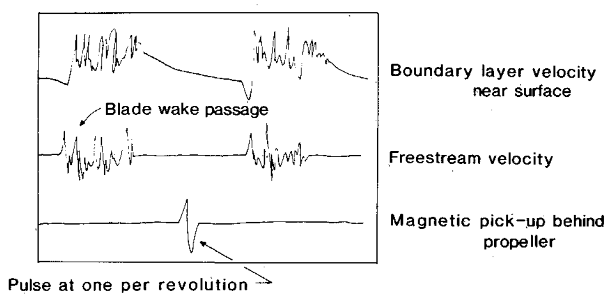

Fig. 8 Conceptual sketch of the wind-tunnel model hot-wire velocity signals.

(higher thrust coefficient) and the viscous wake grows larger, leading to a lengthened impulse disturbance signal. The low-frequency wave pattern which develops in the external slipstream flow results from the helical propeller tip vortex (downwash relative to the blade trailing edge). As demonstrated by Sparks and Miley,[9] the helical tip vortex induces an axial component (blade downwash) in the slipstream velocity which increases in magnitude with vortex strength (propeller thrust coefficient), and as the edge of the slipstream boundary is approached. While the tip-vortex-induced flow dominates the external flow slipstream velocity signal, it is evident that the relatively smaller blade-viscous-wake disturbance affects the laminar boundary layer. In both Figs. 5 and 6, the cyclic disturbances in the flow appear at the frequency of 80 times per second, the blade-passing frequency.

A slipstream boundary-layer interaction disturbance flow model shown in Fig. 7 was constructed from an analysis of the flight and wind tunnel data available. The viscous wake from the propeller blade forms a traveling helical sheet of turbulence which is intersected by the wing. Between these traveling regions of turbulence, regions of laminar flow exist, the lengths of which are dependent upon the degree of local laminar stability and the blade wake characteristics. At a stationary point within the boundary layer, the turbulence in the helical wake appears as large scale, periodic external flow disturbances. The laminar boundary layer responds to these disturbances by locally transitioning to an apparent turbulent state. Other than the induced axial flow velocity pulses, the propeller tip vortex is not apparent in the slipstream disturbance measurements made in these investigations. The tip vortex only comes into contact with the wing surface at the edge of the slipstream and is, therefore, not a part of the disturbance behavior measured in these experiments. There is ample visual evidence, for example, from condensation flow visualization in humid conditions, that the propeller tip vortex structure remains after being split by the wing into upper and lower parts. This conceptual model of the slipstream disturbance interaction with the laminar boundary layer provides an improved understanding of the achievability of laminar flow on airframe surfaces located in propeller wakes.

Wind Tunnel Investigation

A small-scale wind tunnel test program was performed to study the chordwise boundary layer response to propeller slipstreams in more detail. The test model was a 30 in. chord NACA 0012 composite wing section with an 18 in. diam, two-bladed propeller and electric motor mounted at wing level at one-fifth chord distance upstream. Measurements were made at various angles of attack using the same dual-probe hot-wire approach as was used in flight. The probes were traversed in a chordwise direction along the airfoil with the probe support free to pivot allowing the sensors to follow the airfoil contour. The probe heights above the surface were maintained at approximately 0.01 and 1.0 in., respectively.

Hot-wire time history results for two different pressure gradients (angles of attack) are given in Figs. 8–10. Figure 8 is a conceptual sketch of the hot-wire signal behavior to illustrate the significant features appearing in the data. Figure 9 shows the hot-wire signals in the boundary layer and in the external flow within the slipstream, for a favorable pressure gradient extending well back from the leading edge. The upper row of pictures shows velocity time histories at chord locations indicated with the propeller stopped. Transition takes place at approximately 70% chord at a chord Reynolds number of 6×10^5. Low-frequency Tollmien-Schlichting waves appear in the signals with intermittent bursts of turbulence. The lower row of pictures shows the velocity signals with the propeller rotating. The waveform of the cyclic velocity variation begins with the immediate jump to a turbulent velocity level and high-frequency oscillations with the arrival of the external disturbance at the hot-wire station. After the disturbance passes, the velocity returns to the laminar level. The length of the turbulent transitional part of the cycle increases with decreasing laminar stability in the chordwise direction.

With the propeller rotating, the passage of regions of laminar flow occurs further downstream along the chord than occurred with the propeller stopped. This effect can be seen in the figure as far aft as the 80% chord location. This behavior was also observed in the flight data but it is more pronounced here, possibly due to the relatively lower Reynolds number.

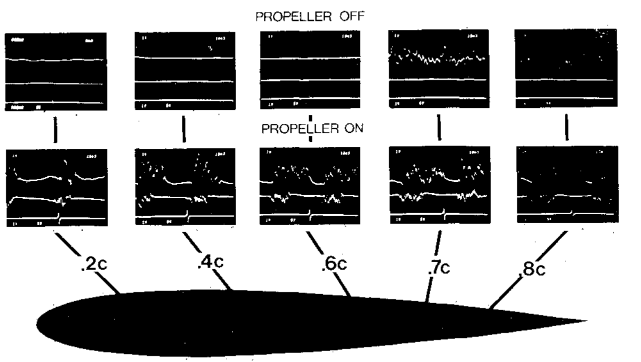

Fig. 9 Time-dependent velocities in boundary layer, favorable pressure gradient.

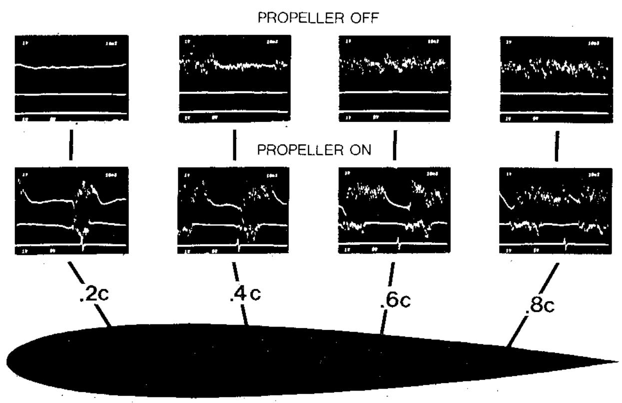

Fig. 10 Time-dependent velocities in boundary layer, adverse pressure gradient.

Figure 10 shows the results for a more adverse pressure gradient. With the propeller stopped, the laminar boundary layer now transitions at 40% chord. The cyclic passage of laminar regions far downstream of the prop-stopped transition location is even more evident for this case. For both of these tests conditions, the propeller slipstream appears to have a potentially beneficial contribution in the pressure recovery region of the airfoil. It is possible that the turbulent transitional process resulting from the external propeller-wake disturbance energizes the flow adjacent to the wall, reducing the momentum defect. Another explanation for the effect is that the propeller wake may create locally favorable pressure gradients which travel with the laminar intervals along the surface, providing sufficient laminar stability to delay transition in the pressure recovery region. The possible presence of a three-dimensional cross flow mechanism in the swirling slipstream was investigated by hot-wire measurements, but no obvious three-dimensional effects were seen. The cyclic laminar/turbulent changes appear to be primarily two-dimensional rather than three-dimensional in this regard.

A second series of wind tunnel experiments was conducted using a single hot-wire probe to traverse the boundary layer normal to the surface. Runs were made at three angles of attack, and velocity time histories were digitized and stored with a microcomputer. Sufficient data were recorded to construct time histories of the time-ensemble velocity and turbulence intensity profiles.

Figure 11 shows three sets of velocity profiles, each set including three profiles at different stages in the wake passage cycle (1/2 revolution of the propeller). The profiles have not been normalized with respect to thickness. Judged by their respective shapes, the velocity profiles vary from a turbulent to a laminar and back to a turbulent profile through a reverse-transitional or laminar-reversion profile.

Analysis and Results

Previous investigations on the effect of external flow turbulence on laminar and turbulent boundary layers have been primarily concerned with heat transfer. Dyban, Epik and Surpun[10] have studied the laminar boundary layer over a flat plate with external flow turbulence intensities ranging up to 25%. The resulting boundary layer velocity and turbulence intensity profiles are similar to those reported herein for the slipstream disturbance case.

What appears to be turbulent flow during the disturbance cycle, is, in fact, not fully developed turbulence, but an intermediate transitional stage, which returns to a laminar condition once the disturbance is removed. The velocity profiles are not within the turbulent range. This point is illustrated in Figs. 12–14 as discussed below.

The energy and momentum thickness parameters H_{32} and H_{12} are ratios of representative boundary layer thicknesses and allow for a classification of velocity profiles for conventional laminar and turbulent flows. For the wind tunnel cases, each time cycle (one blade wake passage) was segmented into 40 parts, and each part was ensemble-averaged over 50 cycles. The resulting velocity profiles were smoothed, fit with a cubic

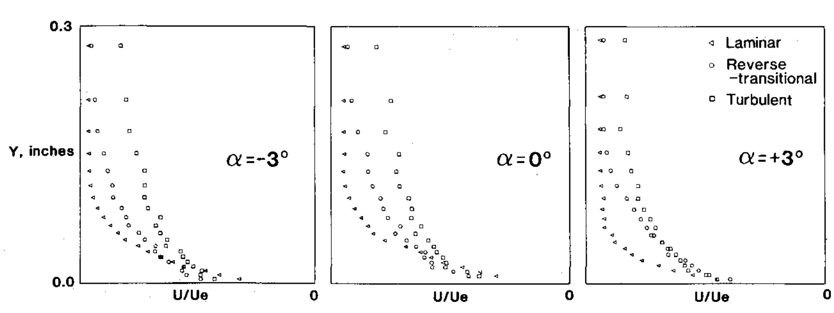

Fig. 11 Bounday layer profiles in the slipstream blade-wake passage cycle.

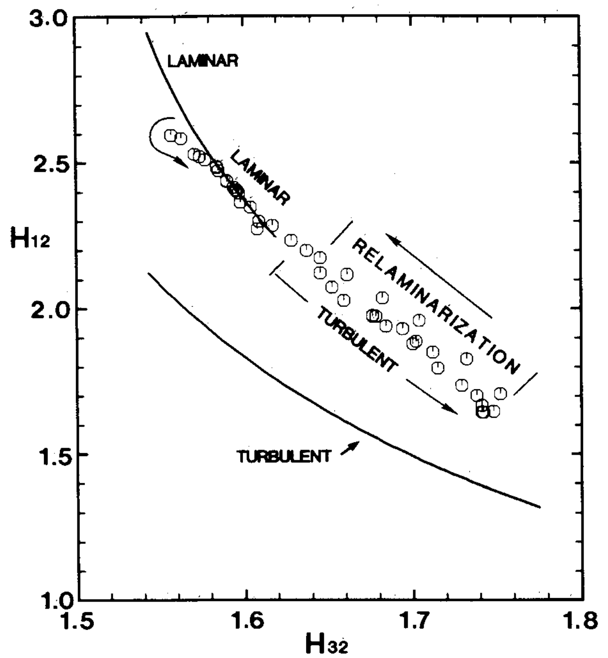

Fig. 12 Shape factor correlation for slipstream flow: 15% chord location.

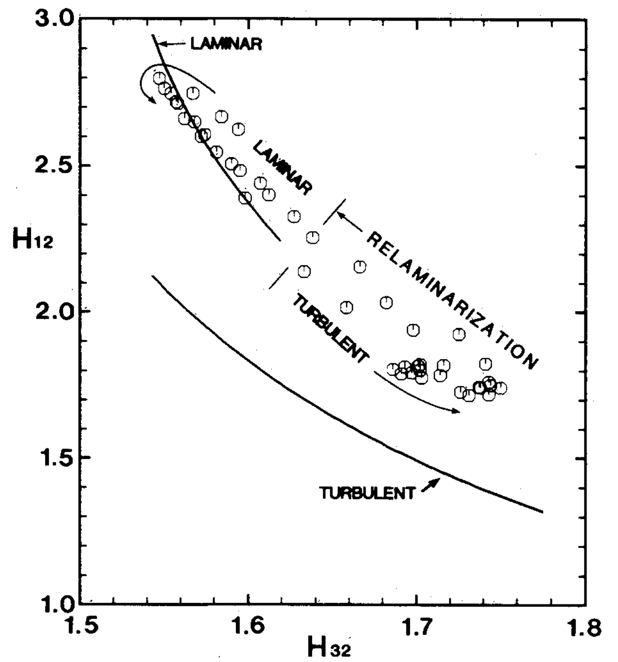

Fig. 13 Shape factor correlation for slipstream flow: 45% chord location.

spline, and integrated for values of H_{12} and H_{32}. The shape factors are plotted and compared with the laminar and turbulent formulations of Eppler[11] as determined from similar solutions and empirical data. Figures 12 and 13 show the shape factor correlation for measurements taken at zero degrees angle of attack and at 15% and 45% chord, respectively. Therefore the results in Fig. 13 are for a more adverse local pressure gradient than in Fig. 12. The boundary layer velocity profiles, as characterized by the shape parameters, never reach the fully developed turbulent range. In Fig. 14, shape parameters for three of the Dyban et al.[10] external turbulence profiles are given. The corresponding external turbulence intensities are noted in the figure. The four percent turbulence point lies close

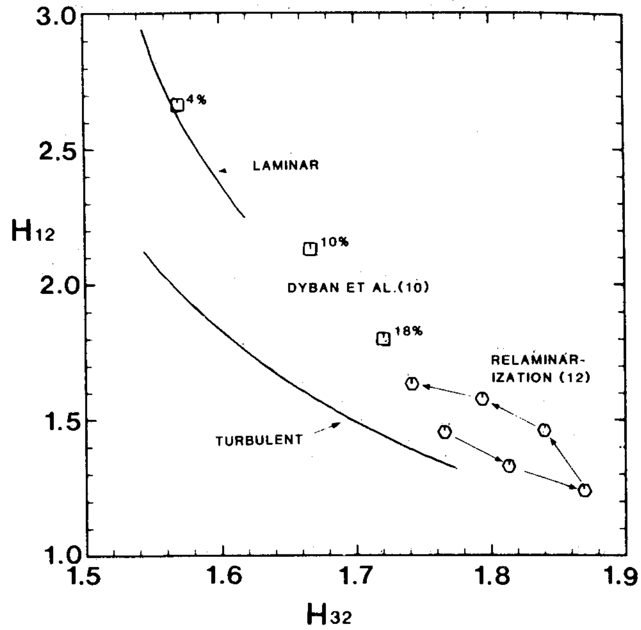

Fig. 14 Comparison of shape factor correlation for laminar flow with external turbulence,[10] and relaminarizing flow.[12]

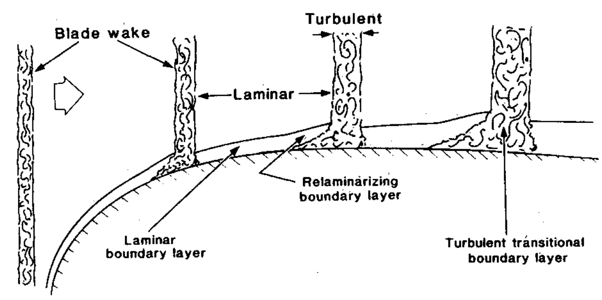

Fig. 15 Present slipstream disturbance flow model.

to the normal flat plate laminar shape parameter value. Increasing external turbulence shifts the points in the same direction as the propeller slipstream disturbance profiles. Also shown in Fig. 14 are points from a relaminarizing boundary layer from Ref. 12. The relaminarizing points imply a path connecting the laminar profile curve with the turbulent profile curve. This path, or at least this region, represents the range of transitional profiles.

These results raise the question of a class of time-dependent boundary layers which is neither laminar nor turbulent. "Relaminarizing" and "reverse-transitional" are terms having a well-defined meaning in the boundary-layer community, referring to a boundary layer that is undergoing a change from turbulent to laminar. The profiles described in this study are convecting profiles and perhaps are better classified as periodic "laminar reversion" boundary layers.

Summary

The laminar boundary layer within a propeller slipstream is affected by the viscous wake from the propeller blade. The wake forms a helical sheet which is split by the wing and passes over the upper and lower surfaces. Across a propeller blade wake passage cycle, the boundary layer at a point on the airfoil surface goes through the distinct phases of laminar, turbulent transitional, and reversion to laminar flow in phase with a cyclic variation in external flow turbulence. This process is illustrated in Fig. 15, which represents the information obtained so far. The turbulent transitional phase is characteristic of boundary layer flow with external turbulence, and exhibits velocity profiles which lie in a transitional region between fully laminar and fully turbulent flow. The cyclic external turbulence may also influence the turbulent boundary layer in such a way as to cause periodic reversion to laminar flow as has been observed in flight and in the wind tunnel.

Acknowledgment

This work was supported by NASA Langley Research Center, Grant No. NAG 1-344.

References

[1]Miley, S. J. and von Lavante, E., "Propeller Propulsion Integration—State of Technology Survey," NASA CR-3882, 1985.

[2]Young, A. D. and Morris, D. E., "Note on Flight Tests on the Effect of Slipstream on Boundary Layer Flow," Aeronautical Research Council R&M No. 1957, 1939.

[3]Young, A. D. and Morris, D. E., "Further Note on Flight Tests on the Effect of Slipstream on Boundary-Layer Flow," Royal Aeronautical Establishment Rept. No. B.A. 1404b, 1939.

[4]Hood, M. J. and Gaydos, M. E., "Effects of Propellers and Vibration on the Extent of Laminar Flow on the NACA 27-212 Airfoil," NACA ACR (WR L-784), 1939.

[5]Zalovcik, J. A., "Flight Investigation of the Boundary Layer and Profile Drag Characteristics of Smooth Wing Sections on a P-47D Airplane," NACA WR L-86, 1945.

[6]Zalovcik, J. A. and Skoog, R. B., "Flight Investigation of Boundary-Layer Transition and Profile Drag of an Experimental Low-Drag Wing Installed on a Fighter-Type Airplane," NACA WR L-94, 1945.

[7]Holmes, B. J., Obara, C. J., and Yip, L. P., "Natural Laminar Flow Experiments on Modern Airplane Surfaces," NASA TP 2256, 1984.

[8]Holmes, B. J., Obara, C. J., Gregorek, G. M., Hoffman, M. J., and Freuhler, R. J., "Flight Investigation of Natural Laminar Flow on the Bellanca Skyrocket II," Society of Automotive Engineers Paper 830717, 1983.

[9]Sparks, S. P. and Miley, S. J., "Development of a Propeller Afterbody Analysis with Contracting Slipstream," Society of Automotive Engineers TP Series 830743, April 1983.

[10]Dyban, Ye. P., Epik, E. Ya., and Surpun, T. T., "Characteristics of the Laminar Boundary Layer in the Presence of Elevated Free-Stream Turbulence," *Fluid Mechanics—Soviet Research*, Vol. 5, July-Aug. 1976, pp. 30-36.

[11]Eppler, R. and Somers, D. M., "A Computer Program for the Design and Analysis of Low-Speed Airfoils," NASA TM 80210, 1980.

[12]Kline, S. J., Cantwell, B. J., and Lilley, G. M., eds., "The 1980-81 AFSOR-HTTM-Stanford Conference on Complex Turbulent Flows: Comparison of Computation and Experiment," Thermosciences Division, Mechanical Engineering Department, Stanford University, Standford, CA, 1981.